Proc. Natl. Acad. Sci. USA
Vol. 96, pp. 7035–7040, June 1999
Neurobiology

Optical recording of light-evoked calcium signals in the functionally intact retina

WINFRIED DENK* AND PETER B. DETWILER†

Bell Laboratories, Lucent Technologies, Murray Hill, NJ 07974

Edited by John E. Dowling, Harvard University, Cambridge, MA, and approved April 5, 1999 (received for review December 23, 1998)

ABSTRACT **Using two-photon excitation of fluorescent indicator dyes, we measured calcium concentration transients in retinal ganglion and amacrine cells without destroying the light sensitivity of the retina by maximally activating or bleaching the photoreceptors. This allowed an immediate assessment of the cellular morphology and study of the calcium signals evoked by visual stimuli. Calcium dynamics in individual dendritic processes could be examined for extensive periods without deterioration and with little apparent phototoxicity at excitation wavelengths of from 930 to 990 nm. Light-evoked increases in calcium were resolved in ganglion- and amacrine-cell neurites, making it possible to use optical recording to study the relationship between calcium signaling and retinal function.**

Signals carried by changes in intracellular calcium play a critical role in the functional state of nearly all cell types. This is certainly true of neurons, in which changes in intracellular calcium concentration ($[Ca^{2+}]_i$) are tightly coupled to the electrical properties of the cell through Ca^{2+}-sensitive ion conductances and voltage-gated Ca channels. Intracellular Ca^{2+} signals also are important in biochemical processes involved, for example, in signal transduction pathways, gene expression (1), and synaptic plasticity (2). As a consequence, the measurement of intracellular calcium transients with the help of fluorescent indicators (3) has become an indispensable tool for the study of electrochemical information processing in neurons and their subcellular compartments.

High-resolution calcium measurements are especially desirable in the retina, where many cells have spatially and electrotonically extensive dendritic trees. The extent of such studies, however, has been limited by the fact that the retina is an exquisite light detector and responds strongly to the light used to excite a fluorescent indicator. As a result, $[Ca^{2+}]_i$ has been measured mainly in either the developing retina, at an early stage before light sensitivity has arisen (4, 5), or in retinal photoreceptors, where the $[Ca^{2+}]_i$ has been estimated before there has been enough time for the $[Ca^{2+}]_i$ changes induced by the excitation illumination to take effect (6–11).

To achieve high temporal and spatial resolution it is necessary to excite fluorescence indicators with light of an intensity that far exceeds that of any natural stimulus. For the calcium indicators that are available currently, the excitation wavelengths lie in a range that also is absorbed strongly by rod and cone visual pigments. Hence, when used in the retina the excitation of fluorescence also excites the photoreceptors and generates a saturating receptor response that persists for as long as the cells are illuminated. This makes the receptors and thus all other retinal neurons blind to visual stimuli delivered during a fluorescence measurement. It, therefore, is not possible to use conventional, i.e., one-photon, fluorescence techniques to continually record light-induced calcium responses in the retina.

Multiphoton fluorescence excitation microscopy (12) has been used to study calcium dynamics in dendrites in brain slices (13, 14) and *in vivo* (15), where improved depth penetration and reduced photodamage are paramount. In this article we demonstrate that by making use of the same underlying principle—the almost complete confinement of molecular excitation to a femtoliter-sized volume—multiphoton fluorescence excitation using infrared illumination permits morphological imaging and spectrofluorometric measurements of calcium dynamics in retinal neurons without concomitant loss of light-evoked responses.

METHODS

Preparation and Electrophysiological Recording. Tiger salamanders (*Ambystoma tigrinum,* larval form; obtained from Charles Sullivan, Nashville, TN) were dark-adapted for an hour or more. The dissection and preparation of the retina was performed under IR illumination (940 nm) with night-vision goggles (NVEC-800HP; Litton, Poly-Scientific, Blacksburg, VA). Retina isolated from a piece of the hemisected eye was placed photoreceptor-side down in a chamber perfused (3 ml/min) with Ringer's solution (110 mM NaCl/22 mM $NaHCO_3$/2.5 mM KCl/1.5 mM $MgSO_4$/1 mM $CaCl_2$/10 mM D-glucose) that was equilibrated with 5% CO_2/95% O_2. To prevent it from moving in the fluid stream the retina was held under a "harp" (made of nylon or gold threads stretched and glued across a U-shaped piece of gold or platinum wire) or clamped on three sides by using springs made from tungsten wire. The preparation was illuminated through a substage condenser with an LED (940-nm wavelength) and observed by using a charge-coupled device video camera (D39244; Edmund Scientific, Barrington, NY). Observation as well as two-photon laser scanning and fluorescence detection were performed through a water-immersion lens (Achroplan, 63×/0.9 WI; Zeiss). Motorized micromanipulators (MP100; Sutter Instruments, Novato, CA) were used to position the microelectrode used for electrical recording as well as a second, "pusher" pipette to help the microelectrode penetrate the internal limiting membrane. The second pipette (opposing or at a right angle to the recording electrode) was used to provide a counterforce that prevented excessive movement of the internal, limiting membrane and distortion of the underlying retinal architecture. The recording electrode was connected to a high-impedance, negative-capacitance amplifier (Axoclamp 2A; Axon Instruments, Foster City, CA), and the output was

The publication costs of this article were defrayed in part by page charge payment. This article must therefore be hereby marked "*advertisement*" in accordance with 18 U.S.C. §1734 solely to indicate this fact.

PNAS is available online at www.pnas.org.

This paper was submitted directly (Track II) to the *Proceedings* office.
Abbreviations: $[Ca^{2+}]_i$, intracellular calcium concentration; LED, light-emitting diode; n.a., numerical aperture.

*To whom reprint requests should be addressed at: Biological Computation Research Department, Room 1C463, Bell Laboratories, Lucent Technologies, 600 Mountain Avenue, Murray Hill, NJ 07974. e-mail: denk@bell-labs.com.
†Present address: Department of Physiology and Biophysics, University of Washington, Seattle, WA 98195.

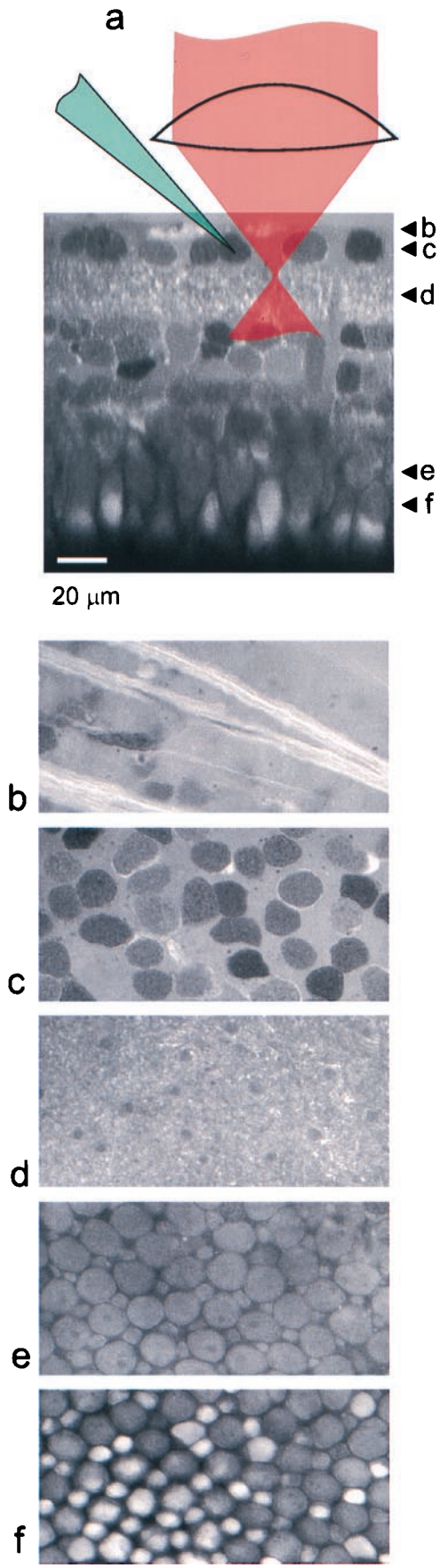

FIG. 1. Optical penetration into the retina. (*a*) *X–Z* section through a retina stained by perfusing with Ringer's solution containing about 0.1 mM soluble fluorescein (catalog no. 16 630–8; Aldrich). *X–Y* sections at various depths: inner limiting membrane with axon bundles, 0 μm (*b*); ganglion cell layer, 10 μm (*c*); inner plexiform layer, 30 μm (*d*); inner segments, 110 μm (e); inner and outer segments, 140 μm below the inner limiting membrane (*f*). (*b–f*) These were taken with the same excitation intensity and are displayed on the same gray scale. Excitation light (930-nm center wavelength) was entering through the objective lens from the ganglion-cell side.

recorded in one of the first few pixels of each scan line to ensure accurate registration with the optical signal. Cell penetration usually was promoted by a brief (<1-ms) burst (buzz) of oscillations caused by capacitance overcompensation. Electrodes were pulled from borosilicate glass capillaries (1-mm o.d./0.5-mm i.d., with filament; Sutter Instruments) on a laser puller (P2000; Sutter Instruments) and had resistances between 250 and 350 MΩ when filled with 300 mM potassium acetate, to which about 5 mM Ca-green 1 or Oregon green 488 BAPTA-1 (both from Molecular Probes) had been added.

Visual Stimulation. Red (λ = 650 nm) and green (λ = 560 nm) light-emitting diodes (LEDs) that illuminated the whole retina were used to deliver full-field light stimuli. Moving bar stimuli were generated by using the beam from a laser pointer (D54006; Edmund Scientific; λ = 635 nm) that was deflected by an *X–Y* pair of galvanometer mirrors (model 6800; Cambridge Technology, Cambridge, MA) and focused onto the retina by using the substage condenser [0.32 numerical aperture (n.a.)]. For local stimulation the same condenser projected a 10-μm spot onto the photoreceptor layer from a pinhole illuminated by a yellow LED (λ = 587 nm).

Laser-scan recording was performed with a custom-built laser-scanning microscope (16) by using a pair of galvanometer mirrors (model 6800HP; Cambridge Technology) driven by custom software. The light source was a Ti:sapphire laser (Tsunami; Spectra-Physics) that provided ≈200-fs pulses at 100 MHz that normally were tuned to 930-nm center wavelength. This wavelength was used to minimize residual one-photon excitation of rod and cone visual pigments and to take advantage of a secondary peak in the two-photon excitation spectrum of the indicator (17). Estimated average laser powers at the retina ranged from 2 to 30 mW. Fluorescence was detected in whole-area mode (18) by using either a photomultiplier tube (R9836; Hamamatsu, Middlesex, NJ) or an intensified photodiode (19) with a fluorescein emission filter. All $[Ca^{2+}]$ dynamics data were acquired in line-scan mode with 2-ms time resolution and were analyzed by using the IDL software package (Research Systems, Boulder, CO).

RESULTS

Optical Penetration into the Retina. The optical properties of the retinal-processing layers are far more favorable than those of other neural tissues. This can be seen in Fig. 1, where Ringer's solution containing fluorescein was used to counterstain the cells in the retina. When imaged from the ganglion cell side, there is little, if any, reduction of fluorescence intensity and image resolution upon traversing from the inner limiting membrane to the outer nuclear layer. Presumably, the biological reason for such optical clarity [which also is responsible for a marked lack of contrast when the retina is viewed with Nomarski differential interference contrast microscopy (DIC) optics] is to avoid scattering the image-forming light as it transverses the retina to reach the photoreceptors. In areas in which the inner limiting membrane had been removed by tearing with the electrodes or was accidentally missing, the ganglion-cell bodies became much more visible with IR transillumination, and we also noticed a severe degradation in the depth penetration for the two-photon fluorescence imaging. In such retinas, unlike those with an undamaged inner limiting membrane, it was impossible to follow the electrode to the outer nuclear layer or image dye-filled horizontal cells. It was

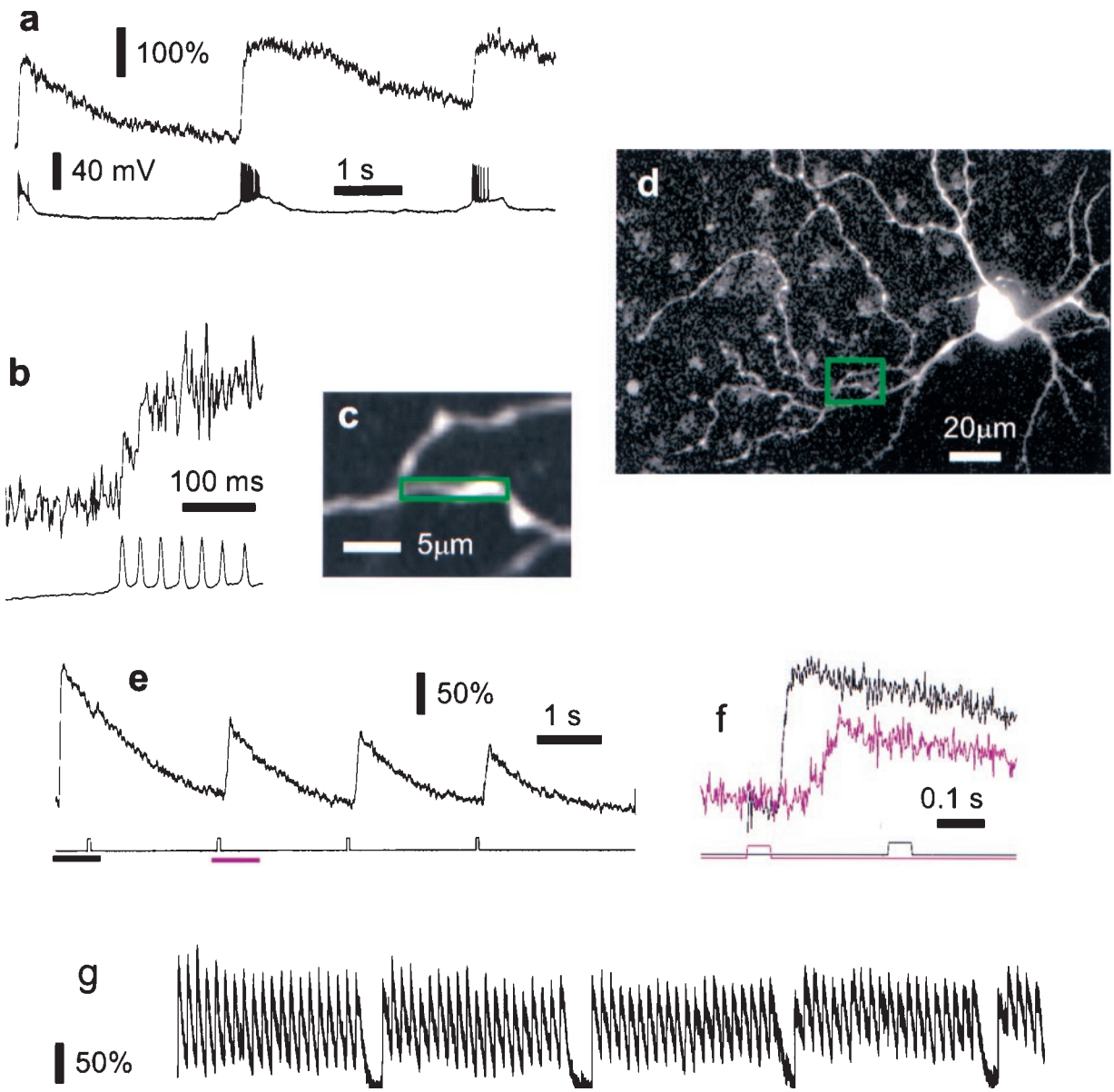

FIG. 2. Light-evoked $[Ca^{2+}]_i$ changes in functional intact retinal ganglion cells. In this cell, after line scanning had commenced, a transient depolarization and a burst of action potentials were seen in response to the laser light used for two-photon imaging (*a Lower*, membrane potential). At the same time a transient calcium rise occurs (*a Upper*, smoothed with a 20-ms sliding time window). As laser line scanning continues, the indicator fluorescence returns to its initial level but rises again during spontaneous bursts of action potentials. At higher time resolution (*b*), the unsmoothed fluorescence trace reveals step-like increases that are coincident with action potentials (vertical scales as in *a*). The area used for the fluorescence measurement is indicated in *c*, and its location relative to the soma is shown in *d*. In a different cell (*e* and *f*) the $[Ca^{2+}]_i$ responses to brief light flashes are suppressed for some time after the start of the scan but recover quickly. In *f*, the time course of the responses in *e* are compared for the initial transient (black trace) and the recovered LED-flash response (magenta trace). The respective LED stimulus traces are shown below. Note that during the initial transient there is no additional response to the LED stimulus. In a third cell (*g*) the response to photic stimulation was virtually unchanged during several minutes of continuous recording from a short dendritic segment (data smoothed with 20-ms sliding window). All cells were filled with Ca-green 1.

also impossible to obtain any useful images, either visually or by laser scanning, when coming from the photoreceptor side. This presumably is due to the laser focus being degraded by the array of microlenses formed by the photoreceptors' outer segments, which have a refractive index that is rather different from the surrounding medium, a fact that also is responsible for their strong DIC contrast.

Morphology. For calcium measurements in individual retinal neurons, fluorescent indicators were introduced by iontophoresis (with currents in the sub-nanoampere range applied for tens of minutes) from sharp microelectrodes, which, at the same time, served to record the cells' membrane potential. Several minutes after first penetrating a cell with a microelectrode, the dendritic morphology became apparent (Fig. 2*d*), which helped to assess the cell type and allowed suitable parts of the dendrite to be selected for recording fluorescence signals.

Imaging Laser Effects. Fig. 2 *a* and *e* shows that transient electrical and calcium responses were triggered in some cells when the imaging laser first started impinging on the retina, but after a few seconds, fluorescence (i.e., $[Ca^{2+}]_i$) and membrane voltage returned to their resting levels. In whole-area scan mode, in particular, if a large field of view was imaged at high resolution leading to a slow frame rate (more that 1 s per frame), cells often responded with periodic spike discharges or subthreshold voltage changes in synchrony with the large area

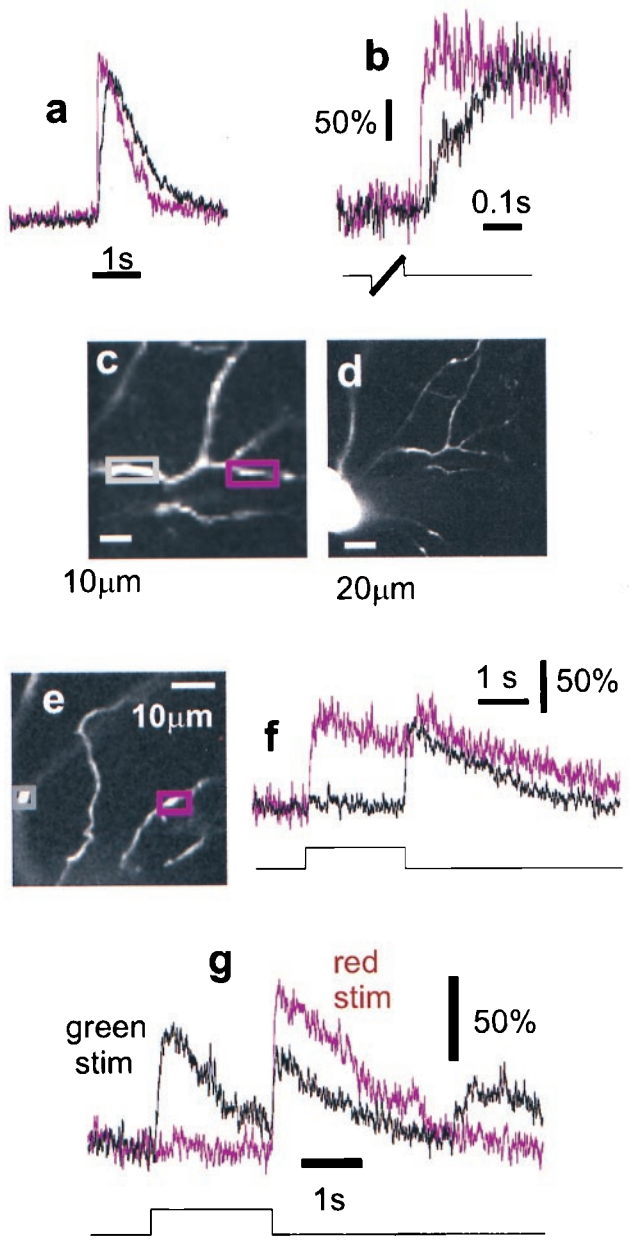

FIG. 3. Intra- and inter-dendritic response variation. Simultaneous measurements (*a* and *b*) in nearby parts of the same dendrite (magenta trace corresponds to magenta box in *c*; for location relative to the soma see *d*) show variations in the temporal profile of the $[Ca^{2+}]$ response. Stimulation was with a moving bar. In *b* the responses are shown at higher time resolution (stimulus light was on during thick part of stimulus trace). Note also in *a* the lack of even a transient response to the imaging laser. $[Ca^{2+}]_i$ dynamics in processes that are spatially close (*e*) but originate from different cells are compared in *f*. The difference in the responses to different color stimuli is shown in *g* for yet another cell. The light intensities were $\approx 20\ \mu W/cm^2$ for the red (650 nm) and $\approx 1\ \mu W/cm^2$ for the green (560 nm) stimulus. For the responses to green light, the response of the fluorescence detector to the stimulus light (not shown, but comparable in size to the fluorescence signal) has been subtracted. All cells were filled with Ca-green 1.

scan (data not shown). To avoid this problem and to achieve high time resolution, all $[Ca^{2+}]_i$ data were taken in line scan mode, which did not cause synchronous membrane potential changes beyond the initial transient. It is likely that the reason for this is that the movement of the beam is fast enough on the time scale of the retinal response to mimic stationary illumination.

For a brief period after the start of the scan, $[Ca^{2+}]_i$ was unresponsive to weak light stimuli (Fig. 2*e*) but stable responses, in this case to full-field stimuli, returned and persisted. Calcium signals were robust and changed little over time even when recording for several minutes from the same region of a dendrite (Fig. 2*g*). Similar responses (data not shown) were evoked by a small spot stimulus located in the center of the scanned area. This demonstrates that during two-photon fluorescence measurements the retinal photoreceptors within the scanned area retain their light sensitivity. The electrical response of a horizontal cell located at the center of the field of view was used to assess the extent of photoreceptor activation caused by the imaging laser. Approximately equivalent horizontal cell responses were evoked by a full-field flash of 650-nm light (150 ms at 150 nW/cm^2) and a single sweep of the imaging laser (64 lines, 2 ms each, covering an area of about 130 $\mu m \times 130\ \mu m$) with an estimated average laser power at the sample of 20 mW. At laser wavelengths of 930 or 990 nm the response to the scan was virtually unaffected by the focal-plane position and was independent of whether the laser was mode-locked, i.e., producing short pulses, or running in continuous-wave mode. These observations strongly indicate that the response to the laser scan mainly is due to one-photon rather than two-photon absorption because two-photon excitation falls off strongly along the *z* axis and mode locking increases the rate of two-photon excitation by about 10^5 (18). When L-cone sensitivity was suppressed, however, by continuous 650-nm full-field illumination, the horizontal cell responses evoked by laser scanning (990-nm wavelength) were dominated by nonlinear absorption, as shown by a strong dependence on mode locking.

Action-Potential Responses. The temporal resolution and signal-to-noise ratio of the measurements were sufficient to detect individual upward steps in the fluorescence signal, coincident with electrically recorded action potentials (Fig. 2*b*). This indicates that in ganglion cells, voltage-gated Ca^{2+} channels are responsible for at least some of the light-induced Ca^{2+} influx. In thin dendritic processes, the increase in $[Ca^{2+}]_i$ reached a maximum after as few as two action potentials (Fig. 2 *a* and *b*). This observation, along with the large size of the relative fluorescence change (20) and its delayed nonexponential falling phase, suggests that the local increase in $[Ca^{2+}]_i$ is enough to saturate the indicator. The final $[Ca^{2+}]_i$ level reached during a burst of action potentials, therefore, could be well into the micromolar range, but for a more direct measurement, indicators that have a lower calcium affinity and, thus, saturate at higher $[Ca^{2+}]_i$ need to be used.

There are also substantial differences in the temporal dynamics of $[Ca^{2+}]_i$ changes in neighboring regions of the same dendritic tree (Figs. 3 *a* and *b*). The $[Ca^{2+}]_i$ rise in the thinner, more distal branch is much faster, and the decay is somewhat accelerated. These differences could be caused, at least partially, by nonuniformity in surface/volume ratio.

Response Variation. Optical recordings can be made from nearby processes belonging to two different cells within the same area if they both are filled with indicator. This is possible because calcium-indicator dyes are retained inside intact cells (21) and most cells survive for many hours after the recording electrode has been withdrawn. The optical recording in Fig. 2*g*, for instance, was made more than 6 h after electrode removal. An example for a comparison between two different cells is shown in Fig. 3 *f* and *g*. One of the processes clearly belonged to an "off" cell and the other one belonged to an "on–off" cell. Because the light-evoked Ca^{2+} signal is retained even during extensive imaging, it is possible to explore and compare the responses to a wide range of stimulus parameters, such as the color of the stimulus light (Fig. 3*h*). The long-term functional integrity of the retina and the stability of the fluorescence measurements allow the distribution of light-evoked $[Ca^{2+}]_i$ responses to be mapped throughout the dendritic arbor. This

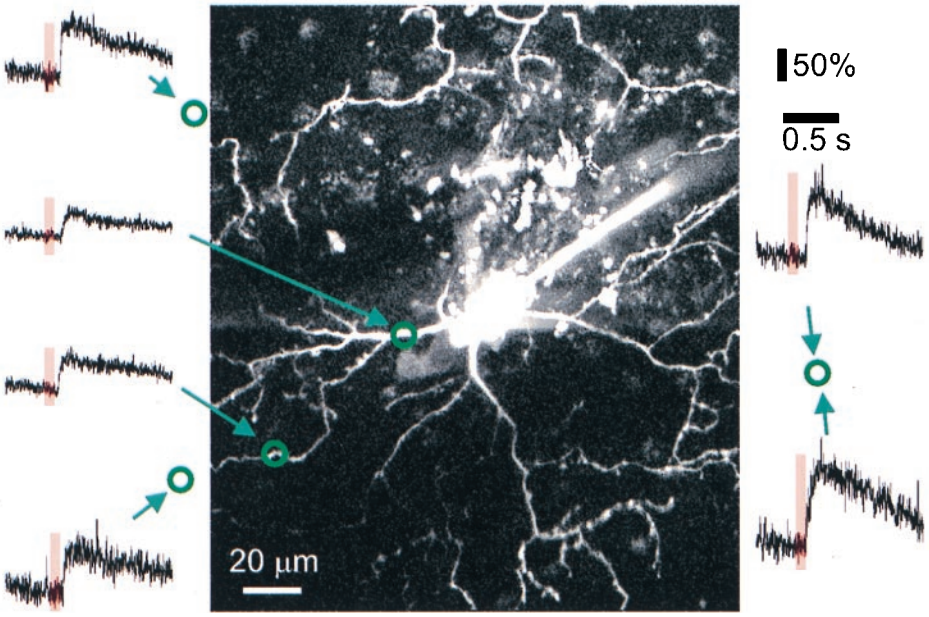

FIG. 4. Map of dendritic $[Ca^{2+}]_i$ responses. Fluorescence changes (Ca-green 1) in response to brief red flashes (650 nm, indicated by bars) measured in line-scan mode (traces) in different parts of the dendritic tree. Locations (measured by using the calibrated translation stage of the microscope) are indicated by the circles in relation to the cell's morphology (maximum projection of image stack).

is illustrated in Fig. 4, which shows $[Ca^{2+}]_i$ signals in different parts of the dendritic tree of a single neuron in response to brief, full-field flashes of red light.

Amacrine Cell Responses. In a few cases cells with their somata in the inner nuclear layer were recorded that had stable resting potentials and gave $[Ca^{2+}]_i$ responses to small spot stimuli that increased with stimulus intensity (Fig. 5). Different regions of the dendritic arbor could show marked spatial variations of the $[Ca^{2+}]_i$ response to full-field stimuli even when separated by distances of less than 10 μm. Desynchronized spontaneous transients also were observed in neighboring regions of the same dendrite, suggesting that in these cell types, $[Ca^{2+}]_i$ signals may be highly localized (data not shown).

DISCUSSION

We have demonstrated that two-photon excitation fluorescence microscopy can be used to record calcium dynamics in dendritic processes in the isolated retina without photodynamic damage to the cell and without destroying the retina's light sensitivity.

The residual response (Fig. 2) to the pulsed infrared light used for two-photon excited fluorescence imaging is dominated by one-photon absorption as far out as 990 nm as long as the L-cones are active. This may not hold for mammalian retina, where spectral sensitivity of L-cones (22) is shifted substantially toward shorter wavelengths compared with the salamander (23).

The rate of photoisomerization caused by direct two-photon absorption can be estimated only with difficulty, because of the uncertainty in the absolute two-photon cross-sections of visual pigments. Earlier measurements on visual pigment analogs yielded rather high values (24) (>100 GM; 1 GM = 10^{-58} $m^4 \cdot s$), but more recent measurements, using the activation of the phototransduction cascade as an assay, yielded much smaller values (<1 GM) (M. Gray-Keller, W.D., B. Shraiman, and P.B.D., unpublished results). Our experimental finding that after elimination of the L-cone sensitivity the response to the imaging laser became dependent on the mode-lock status indicates a nonlinear optical process. This might involve direct, two-photon absorption by the visual pigments but also could arise from optical second-harmonic generation (25) in the tissue and subsequent reabsorption by photopigments. In particular, before studies of the calcium dynamics in the scotopic regime can be undertaken, the nature and origin of the residual excitation need to be better understood.

Photoreceptor activation by two-photon absorption depends on the distance of the focal plane from the photoreceptor layer. Thus, when imaging deeper in the retina a higher level of photoreceptor excitation by two-photon absorption is to be expected. Measurements in the outer plexiform layer therefore may be complicated or even prohibited by bleaching of photopigment or saturation of the receptor response. The two-photon absorption-induced response depends also on the inverse fourth power of the n.a. (or, in the case of underfilling by the scanning laser beam, on the effective n.a.) of the objective lens, making the use of the highest possible objective n.a. and a proper filling of the back aperture desirable.

Another potential pathway of unintentionally activating the retinal light response is photoreceptor excitation by the emitted fluorescence. Because of large variations in dye concentrations, quantum efficiency, accessible volume, and cell-geometrical factors, it is difficult to estimate accurately the generated fluorescence from the excitation parameters. One can estimate instead, however, the amount of fluorescence needed to obtain sufficient signal-to-noise ratio (S/N) for the measurements. To achieve a photon shot noise-limited S/N of 10, $(S/N)^2$, i.e., 100 photons have to be detected per time point (2 ms). With a typical overall detection efficiency of about 1%, a total generation rate of about 5×10^6 photon/s is required. This corresponds to a power of 2 pW (20 nW/cm^2 in the photoreceptor plane), which is much smaller than the visible-light equivalent of the one-photon direct activation as measured above.

We expect that the technique presented in this paper also will be usable with fluorescent indicators sensitive to the concentration of other intracellular ions, such as Na^+ (26), or second messengers, such as cAMP (27). Particularly powerful, in the retina and elsewhere, should be the combinations of multiphoton imaging with emerging green fluorescent protein-based, genetically encoded fluorescence indicators (28–31). Such probes, in addition to permitting the labeling of many cells at once, also can be targeted to genetically defined subpopulations of cells (32), which will make information

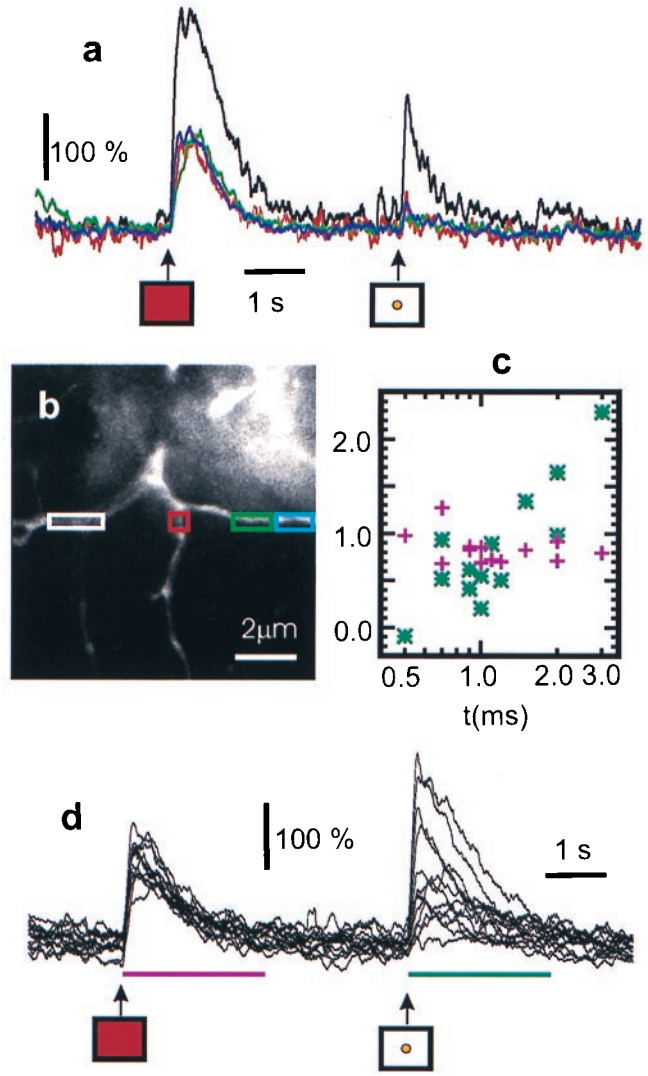

FIG. 5. Spatially inhomogeneous responses in an amacrine cell filled with Oregon green 1,2-bis(2-aminophenoxy)ethane-*N,N,N′,N′*-tetraacetate-1 (*a* and *b*). A red whole-field stimulus (1-ms duration) is followed after 4-s delay by a yellow spot stimulus (5 ms). The spot triggers a $[Ca^{2+}]$ rise in only one branch. Graded response (*d*) in a more distal branch. The duration of the spot stimulus was varied from 0.0 to 3 ms. The resulting responses are plotted in *c* (green asterisks; integrated increases are in units of ΔF·s). The response to the control prestimulus (red, whole-field; 50 μs) remained unchanged (*d*, purple crosses). For both *a* and *d*, the traces were smoothed with a 100-ms sliding window and start 3 s after the scan began.

processing by specific populations of neurons more easily observable. Furthermore, because $[Ca^{2+}]_i$ changes can occur without the generation of action potentials (13), two-photon calcium recording should complement nicely electrode array measurements (33) for population recordings.

We are grateful for advice from David Copenhagen, Markus Meister, John McReynolds, Geoff Owen, and Frank Werblin as well as for support from the National Institutes of Health (Grant EY02048). Ray Stepnoski at Lucent Technologies wrote the laser-scanning software.

1. Deisseroth, K., Heist, E. K. & Tsien, R. W. (1998) *Nature (London)* **392,** 198–202.
2. Malenka, R., Kauer, J., Zucker, R. & Nicoll, R. (1988) *Science* **242,** 81–84.
3. Grynkiewicz, G., Poenie, M. & Tsien, R. Y. (1985) *J. Biol. Chem.* **260,** 3440–3450.
4. Wong, R. O., Chernjavsky, A., Smith, S. J. & Shatz, C. J. (1995) *Nature (London)* **374,** 716–718.
5. Feller, M. B., Wellis, D. P., Stellwagen, D., Werblin, F. S. & Shatz, C. J. (1996) *Science* **272,** 1182–1187.
6. Korenbrot, J. I., Ochs, D. L., Williams, J. A., Miller, D. L. & Brown, J. E. (1986) *Soc. Gen. Physiol. Ser.* **40,** 347–363.
7. Ratto, G. M., Payne, R., Owen, W. G. & Tsien, R. Y. (1988) *J. Neurosci.* **8,** 3240–3246.
8. Gray-Keller, M. P. & Detwiler, P. B. (1994) *Neuron* **13,** 849–861.
9. McCarthy, S. T., Younger, J. P. & Owen, W. G. (1994) *Biophys. J.* **67,** 2076–2089.
10. Younger, J. P., McCarthy, S. T. & Owen, W. G. (1996) *J. Neurophysiol.* **75,** 354–366.
11. Sampath, A. P., Matthews, H. R., Cornwall, M. C. & Fain, G. L. (1998) *J. Gen. Physiol.* **111,** 53–64.
12. Denk, W., Strickler, J. H. & Webb, W. W. (1990) *Science* **248,** 73–76.
13. Yuste, R. & Denk, W. (1995) *Nature (London)* **375,** 682–684.
14. Denk, W., Sugimori, M. & Llinas, R. (1995) *Proc. Natl. Acad. Sci. USA* **92,** 8279–8282.
15. Svoboda, K., Denk, W., Kleinfeld, D. & Tank, D. (1997) *Nature (London)* **385,** 161–165.
16. Denk, W. & Svoboda, K. (1997) *Neuron* **18,** 351–357.
17. Xu, C. & Webb, W. W. (1996) *J. Optical Soc. Am. B* **13,** 481–491.
18. Denk, W., Piston, D. W. & Webb, W. W. (1995) in *The Handbook of Confocal Microscopy*, ed. Pawley, J. (Plenum, New York), pp. 445–458.
19. La Rue, R. A., Edgecumbe, J. P., Davis, G. A., Gospe, S. & Aebi, V. (1993) *SPIE Proc.* **2022,** 64–73.
20. Denk, W., Holt, J. R., Shepherd, G. M. G. & Corey, D. P. (1995) *Neuron* **15,** 1311–1321.
21. Regehr, W. G., Connor, J. A. & Tank, D. W. (1989) *Nature (London)* **341,** 533–536.
22. Rodieck, R. (1973) *The Vertebrate Retina* (Freeman, San Francisco).
23. Makino, C. L. & Dodd, R. L. (1996) *J. Gen. Physiol.* **108,** 27–34.
24. Birge, R. R. (1990) *Annu. Rev. Phys. Chem.* **41,** 683–733.
25. Boyd, R. W. (1992) *Nonlinear Optics* (Academic, Boston).
26. Minta, A. & Tsien, R. Y. (1989) *J. Biol. Chem.* **264,** 19449–19457.
27. Adams, S. R., Harootunian, A. T., Buechler, Y. J., Taylor, S. S. & Tsien, R. Y. (1991) *Nature (London)* **349,** 694–697.
28. Miyawaki, A., Llopis, J., Heim, R., McCaffery, J. M., Adams, J. A., Ikura, M. & Tsien, R. Y. (1997) *Nature (London)* **388,** 882–887.
29. Romoser, V. A., Hinkle, P. M. & Persechini, A. (1997) *J. Biol. Chem.* **272,** 13270–13274.
30. Siegel, M. S. & Isacoff, E. Y. (1997) *Neuron* **19,** 735–741.
31. Miesenbock, G., De Angelis, D. A. & Rothman, J. E. (1998) *Nature (London)* **394,** 192–195.
32. Nirenberg, S. & Meister, M. (1997) *Neuron* **18,** 637–650.
33. Meister, M., Pine, J. & Baylor, D. A. (1994) *J. Neurosci. Methods* **51,** 95–106.